Electronic Supplementary Material (ESI) for Green Chemistry.
This journal is © The Royal Society of Chemistry 2019

Granular fermentation enables high rate caproic acid production from solid-free thin stillage.

Supplementary information

José María Carvajal-Arroyo[a], Pieter Candry[a], Stephen J. Andersen[a], Ruben Props[a], Thomas Seviour[b], Ramon Ganigué[a] and Korneel Rabaey[a,*]

[a]Center for Microbial Ecology and Technology (CMET), Department of Biotechnology, Ghent University, Coupure Links 653, B-9000 Gent, Belgium

[b]Singapore Centre of Environmental Life Sciences Engineering (SCELSE), Nayang Technological University, Singapore, Singapore.

***Corresponding author**

Korneel Rabaey, Ghent University; Faculty of Bioscience Engineering; Center for Microbial Ecology and Technology (CMET); Coupure Links 653; B-9000 Gent, Belgium; phone: +32 (0)9 264 59 76; fax: +32 (0)9 264 62 48; E-mail: Korneel.Rabaey@ugent.be; Webpage: www.cmet.ugent.be.

Analytical methods

COD was analyzed with Nanocolor® kits COD15000, and measured in a photometer Nanocolor 500D (Macherey-Nagel, Düren, GE). Total carbohydrates was analyzed and calibrated with a glucose standard, as in Nielsen et al. (2010).Carboxylic acids (2-8 carbon length), excluding lactic acid and including isoforms C4-C6) were analyzed by gas chromatography (GC-2014, Shimadzu®, NL) with a flame ionization detector (FID). The column was a with DB-FFAP 123-3232 column (30m x 0.32 mm x 0.25 µm; Agilent, BE). Liquid samples were conditioned with sulfuric acid and sodium chloride and 2-methyl hexanoic acid as internal standard for quantification of further extraction with diethyl ether. Prepared sample (1 µL) was injected at 200ºC with a split ratio of 60 and a purge flow of 3 mL min^{-1}. The oven temperature increased by 6ºC min^{-1} from 110ºC to 165ºC where it was kept for 2 min. FID had a temperature of 220ºC. The carrier gas was nitrogen at a flow rate of 2.49 mL min^{-1}. Lactic acid was determined in a 930 Compact IC Flex (Metrohm, CH) ion chromatography system. Separation occurred at 35°C in a Metrosep organic acids 250/7.8 column, equipped with a metrosep organic acids guard column/4.6. Detection was done with a 850 IC conductivity detector (Metrohm, CH). The anions were eluted with H_2SO_4 1mM at a flow rate of 0.5 mL min^{-1}. Ethanol and glycerol were analyzed using a 930 Compact IC Flex (Metrohm, Switzerland) ion chromatography system. Separation occurred at 35 °C on a Metrosep Carb 2 (250/4.0) column with a Metrosep Trap 1 100/4.0 guard column. The eluent was 20 mM NaOH at a flow rate of 0.8 mL min^{-1}. An IC amperometric detector (Metrohm, CH) was used for detection of eluted components. The sample aspiration needle was cleaned with acetone between each analysis. The gas phase composition was analyzed with a Compact GC (Global Analyser Solutions, Breda, The Netherlands), equipped with a Molsieve 5A pre-column and Porabond column (CH_4, O_2, H_2 and N_2) and a Rt-Q-bond pre-column and column (CO_2, N_2O and H_2S). Concentrations of gases were determined by means of a thermal conductivity detector.

Scanning electron microscopy

The granules were fixed as follows: A sample containing 3-4 granules was washed using a Na_2HPO_4 buffer solution (200 mM) at pH 7.2 for 10 min. Subsequently the granules were fixed in a solution containing Na_2HPO_4 (100 mM), glutaraldehyde (2.5%, w v^{-1}) and lysine (75 mM), at pH 7.2, at room

temperature for 20 min. A second fixation step was performed in a similar solution without lysine, for 60 min, after which the granules were washed twice in P buffer (100 mM, pH 7.2) in 10 min steps and subjected to a dehydration series (10 min per step) in ethanol (50%, 70%, 80%, 90%, 95% and 100%, v v^{-1}). Chemical drying was done by submerging the granules in hexamethyldisilazane twice, 30s each. After this, granules were left to air dry for 3h.

Molecular analysis

DNA extraction was performed by means of bead beating with a PowerLyzer instrument (MoBio) and phenol/chloroform extraction[2]. The 16S rRNA gene V3-V4 hypervariable regions were amplified by PCR using primers 341F (5'-CCT ACG GGN GGC WGC AG -3') and 785Rmod (5'-GAC TAC HVG GGT ATC TAA KCC-3'). The reverse primer was adapted from Klindworth et al. (2013), to increase coverage. Quality control PCR was performed using Taq DNA Polymerase with the Fermentas PCR Kit according to the manufacturer specifications (Thermo Fisher Scientific, Waltham, MA, USA). The obtained PCR product was ran along the DNA extract on a 2% agarose gel for 30 minutes at 100V. 10µl of the original genomic DNA extract was send out to LGC genomics GmbH (Berlin, Germany) for library preparation and sequencing on an Illumina Miseq platform with v3 chemistry with the primers mentioned above. To assess the sequencing quality a mock community was included in triplicate in the sequencing run. Read assembly and cleanup was largely derived from the MiSeq SOP described by the Schloss lab [4, 5]. In brief, mothur (v. 1.39.5) was used to assemble reads into contigs, perform alignment-based quality filtering (alignment to the mothur-reconstructed SILVA SEED alignment, v. 123), remove chimeras, assign taxonomy using a naïve Bayesian classifier[6] and SILVA NR v128 and cluster contigs into OTUs at 97% sequence similarity. All sequences that were classified as Eukaryota, Archaea, Chloroplasts and Mitochondria were removed. Also, if sequences could not be classified at all (even at (super)Kingdom level) they were removed. For each OTU representative sequences were picked as the most abundant sequence within that OTU.

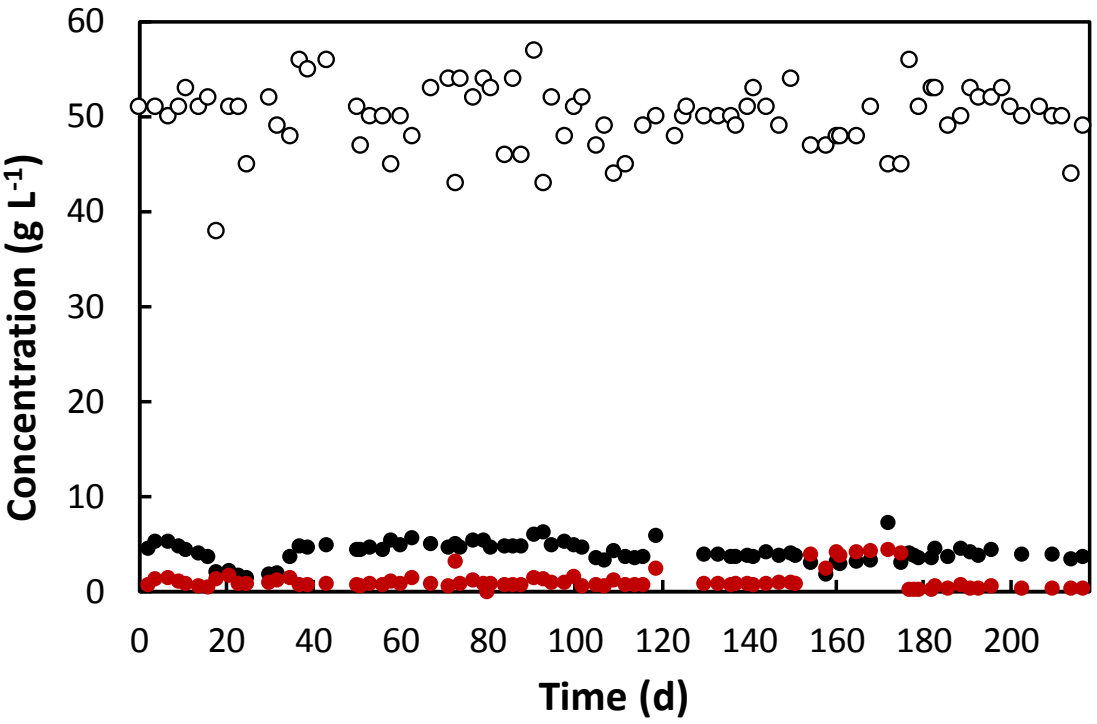

Figure S1. Variability of feed characteristics: influent COD (open symbols), acetic acid (closed red symbols) and lactic acid (closed black symbols) concentrations.

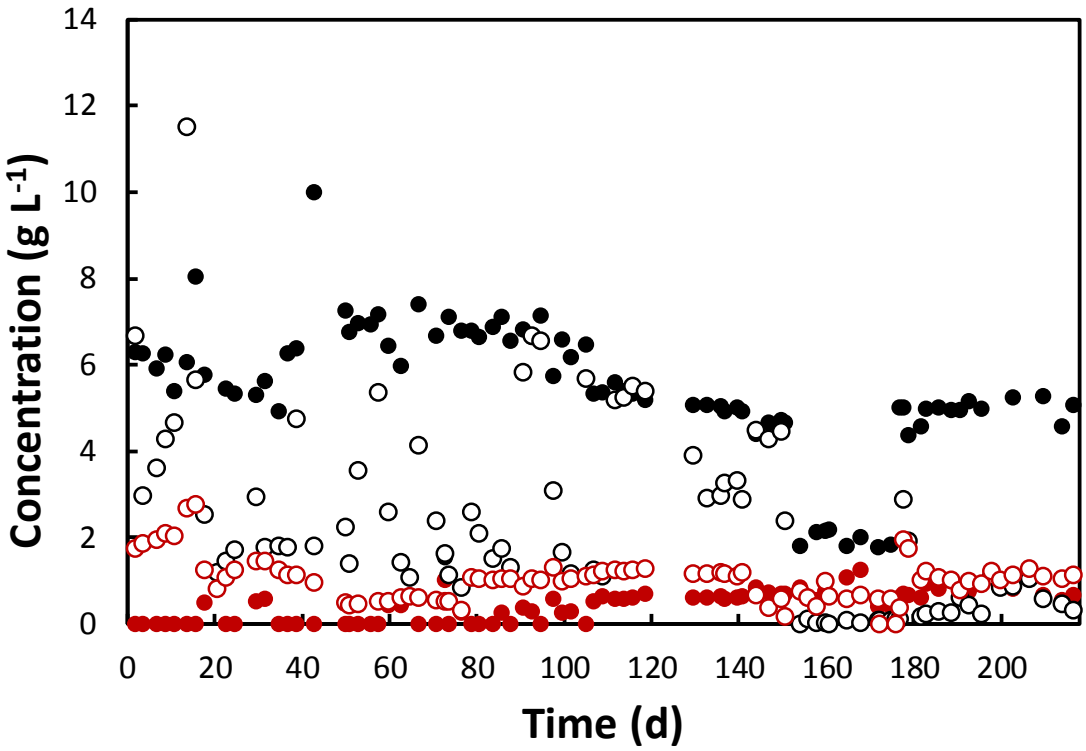

Figure S2. Time course of the concentration of ethanol (red) and glycerol (black) in the feed (closed symbols) and effluent (open symbols) of the granular reactor.

Table S1. Hydraulic retention time during the different periods of the experiment

Experimental period	HRT (d)
0-9	3.9±1.1
10-29	1.7±0.1
30-54	0.8±0.1
55-122	0.6±0.1
123-178	0.4±0.2 (unstable period, min HRT=0.2 d)
179-191	0.8±0.1
192-198	0.5±0.0
198-217	0.4±0.0

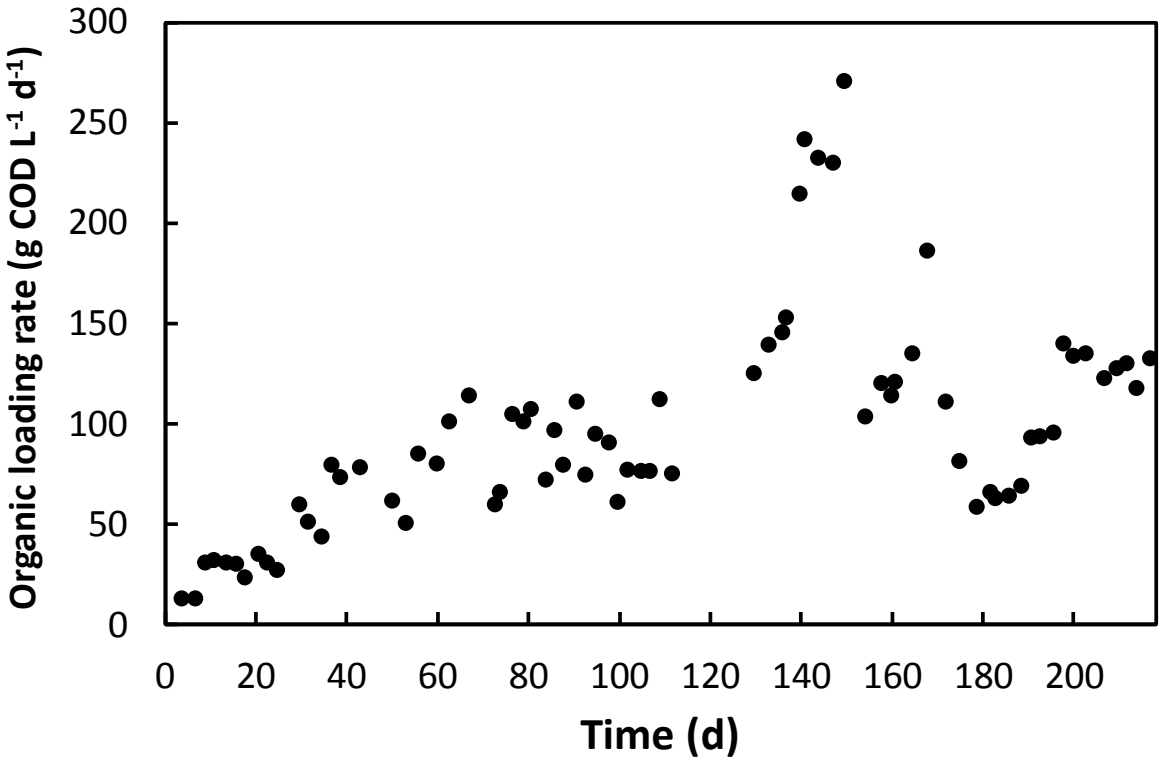

Figure S3. Organic loading rate during the complete experiment.

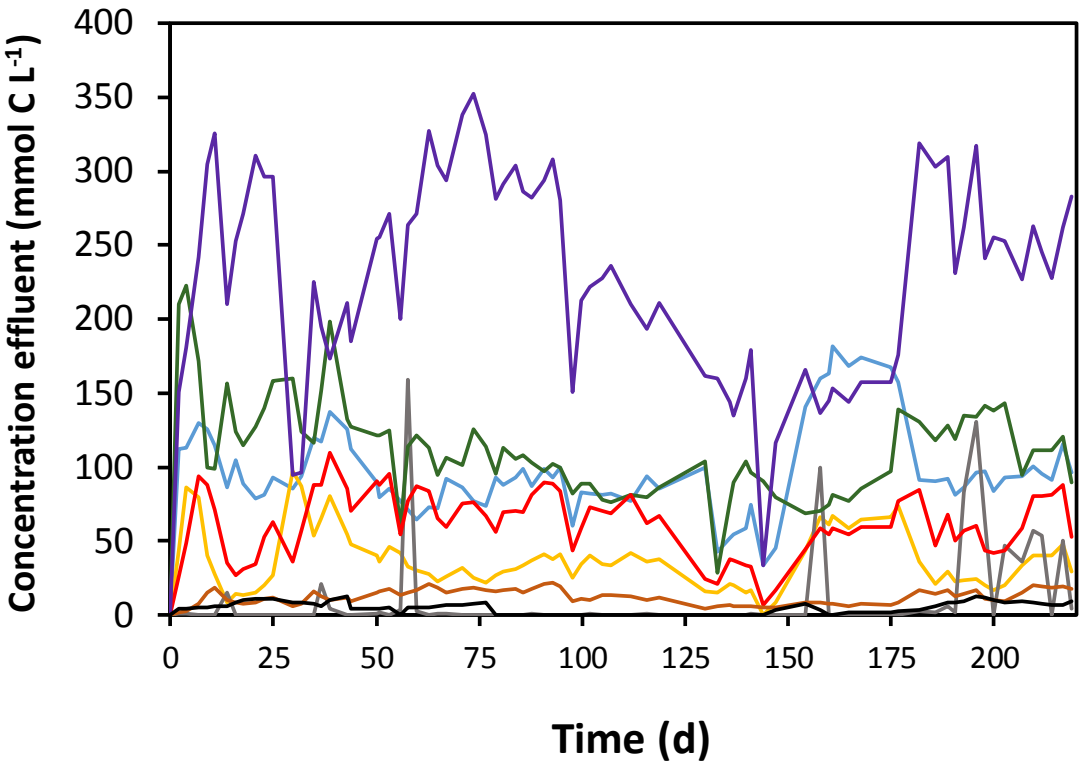

Figure S4. Time course of the evolution of concentration of lactic acid (grey) acetic acid (blue), propionic acid (yellow), n-butyric acid (green), n-valeric acid (red), n-caproic acid (purple), n-heptanoic acid (orange) and n-caprylic acid (black) in the effluent of the fermenter.

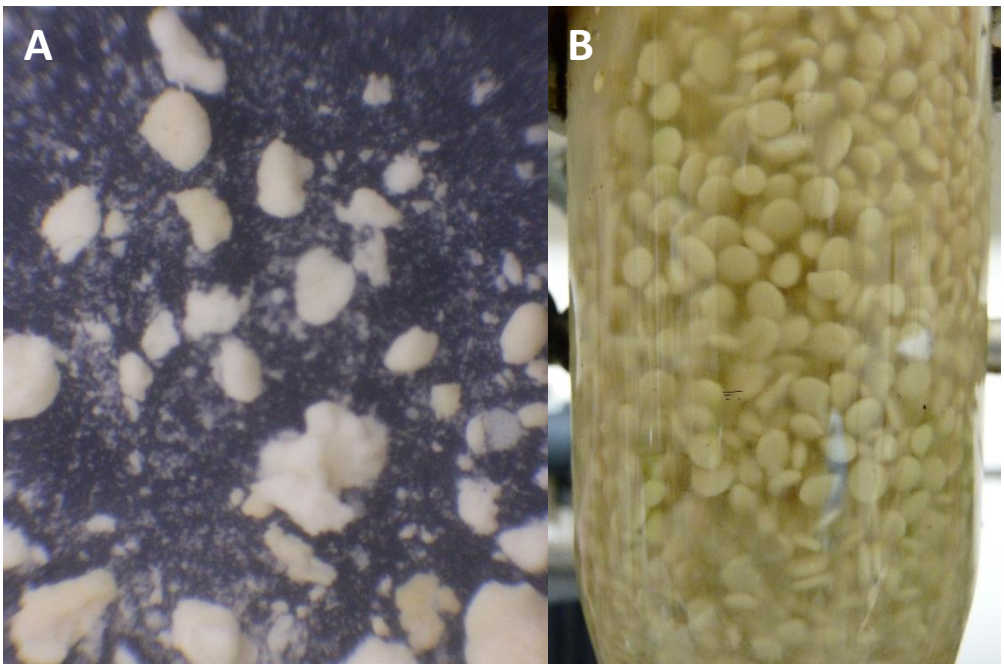

Fig S5. Images of chain elongating granules taken on day 120 (A) and on day 130 (B).

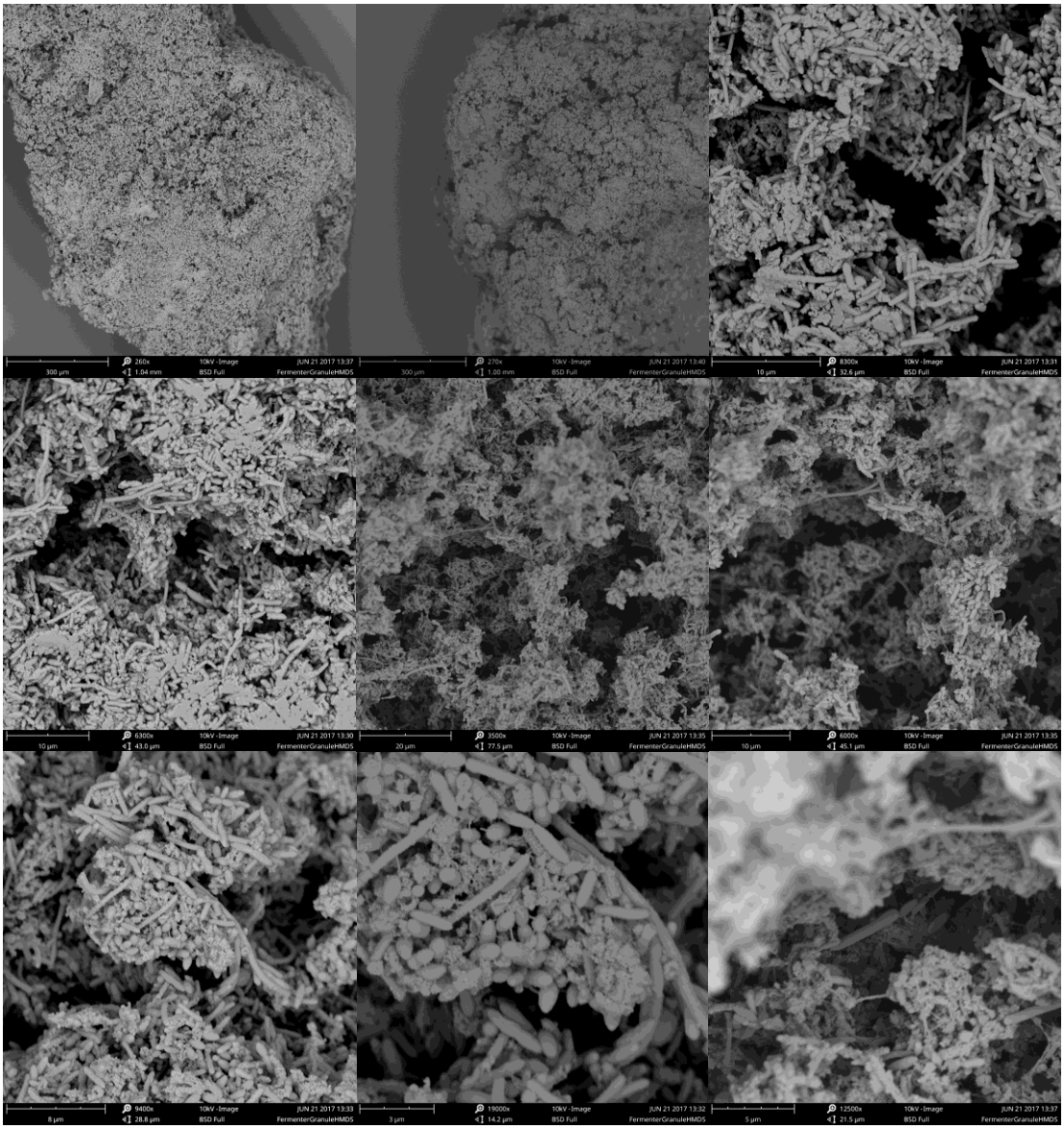

Fig S6. SEM Images of the chain elongating granules sampled on day 33.

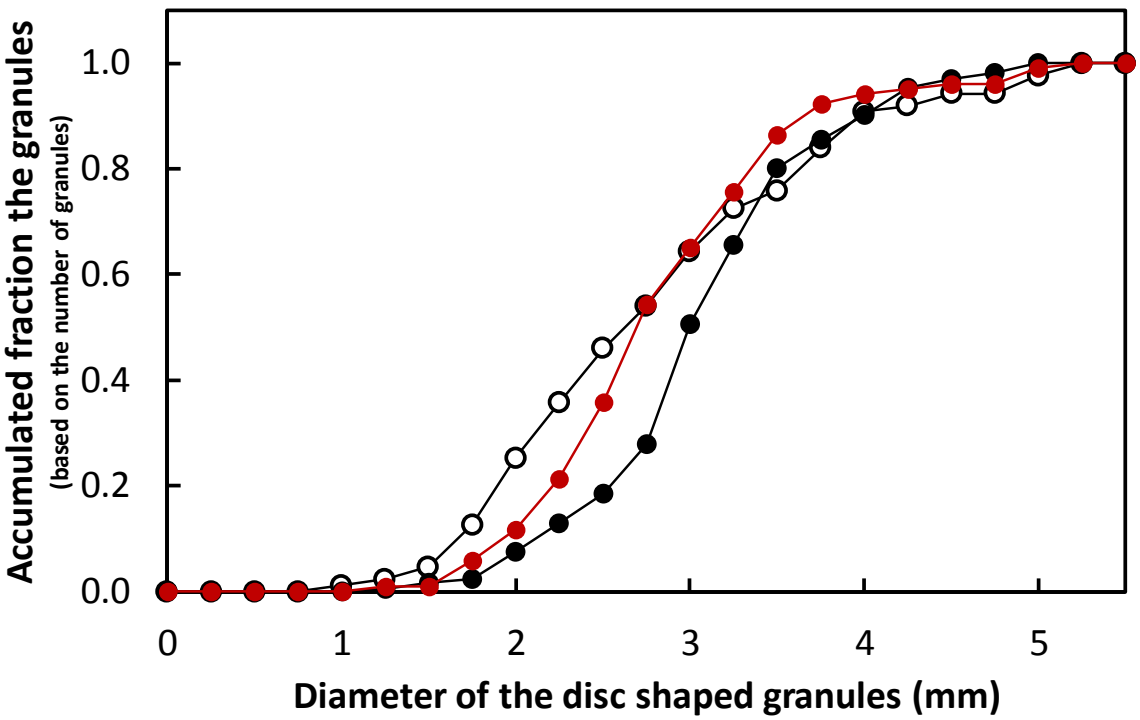

Figure S7. Particle size distribution of the granules sampled on day 130 (open symbols), day 183 (black closed symbols), and day 189 (closed red symbols).

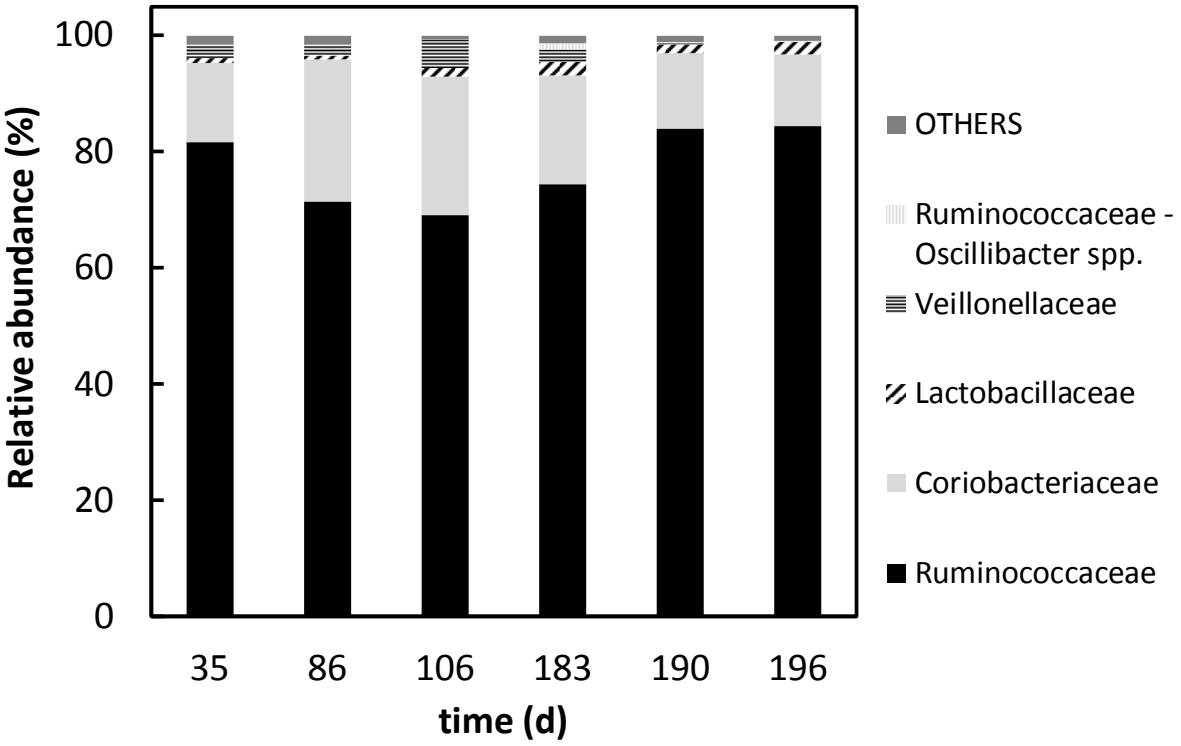

Figure S8. Evolution of the microbial composition of the chain elongating granules.

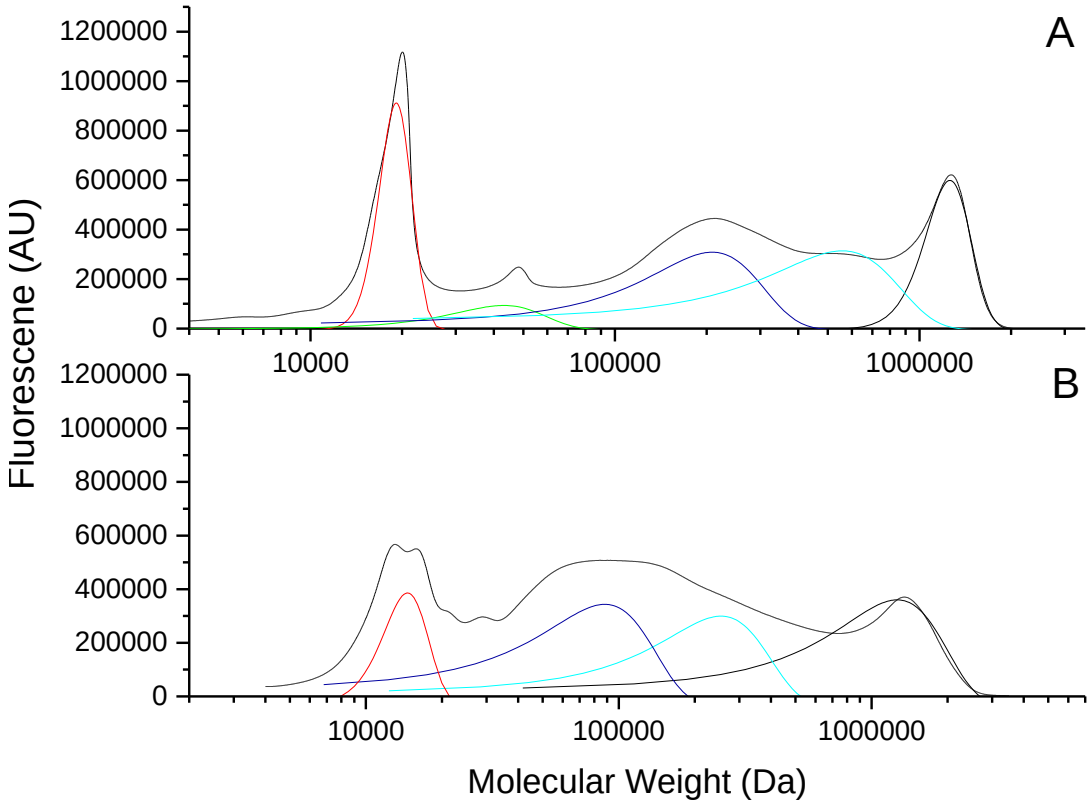

Figure S9. Molecular weight (MW) profiles (black) of freeze-dried crude EPS from granular (A) and suspended (B) sludges. Chromatographic peaks of constituent molecules, estimated by fitting the chromatograms to a Gaussian model, are shown in colored lines. Elution of heparin MW standards were used to convert chromatography retention times into MW. Molecular detection is by fluorescence. Chromatograms were recorded in 0.001 M NaOH at 22 °C.

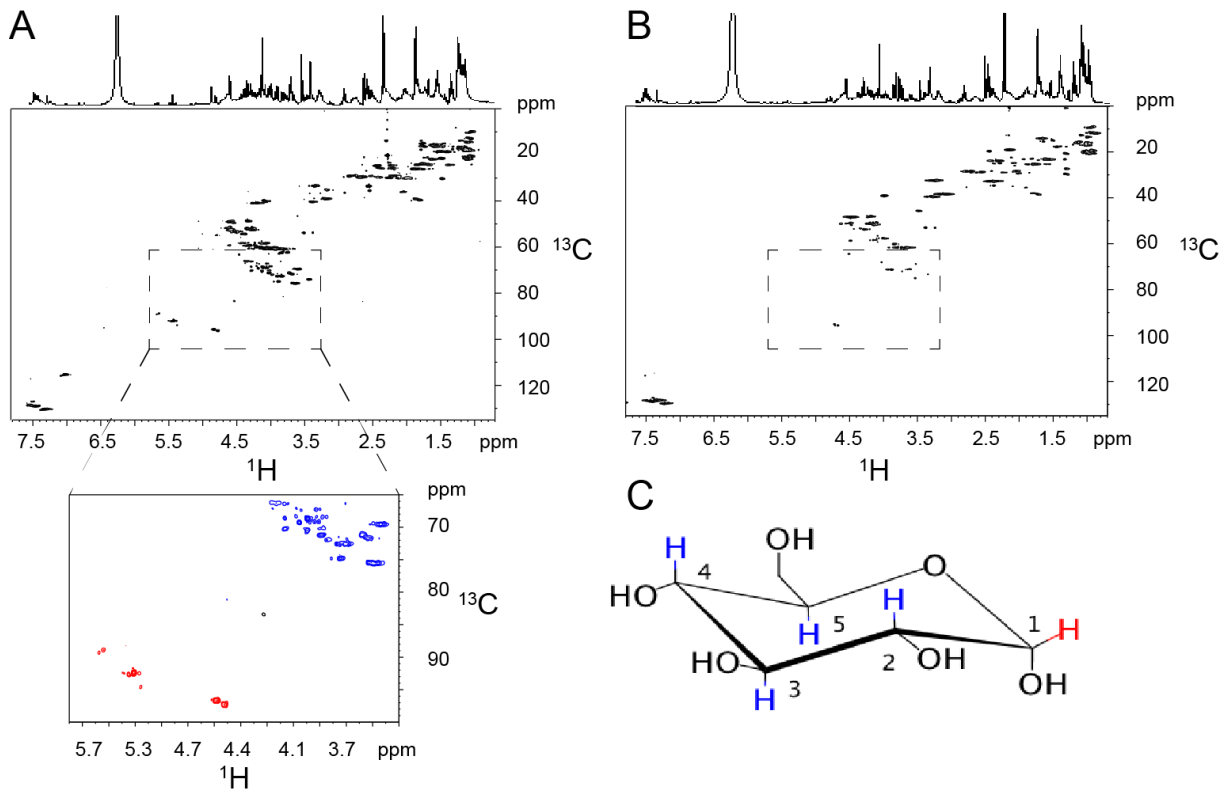

Figure S10. ^{1}H-^{13}C heteronuclear single quantum coherence (HSQC) NMR spectrum of crude granular (A) and suspended (B) sludges digested for 4 hours in 2 M trifluoroacetic acid at 120 °C. All spectra were recorded at 22 °C Cut-out of (A) shows ^{1}H-^{13}C cross-peaks corresponding to anomeric (red) and bulk (blue) sugar H-C couplings. Schematic illustrates numbering across the hexose (in this case glucose) spin system

Table S2. Details of spin-systems identified from ^{1}H-^{31}C HSQC spectra of sludge fractions.

Putative sugar spin system	Proton shift δ_H (ppm)	Carbon shift δ_C (ppm)	Putative H1-H2 coupling constant (Hz)	Relative Abundance (%)		Probable base sugar
				Granular	Suspended	
1	4.67	96.2	8.0	38.6	35.0	β-glucose/ β-galactose
2	4.73	95.7	7.8	21.1	38.4	β-glucose/ β-galactose
3	5.26	93.9	1.6	4.6	4.1	α-mannose
4	5.31	92.0	3.8	20.4	8.3	α-glucose/ α–galactose
5	5.35	92.1	3.4	7.3	7.5	α-glucose/ α–galactose
6	5.53	88.9	3.6	8.0	6.7	α-glucose/ α-galactose

Table S3. Reference species utilized to build the phylogenetic placement tree. Only sequences of the 16S RNA gene where used.

Reference species	**Accession number**
Clostridium kluyveri DSM 555	NC_009706
Clostridium ljungdahlii DSM 13528	CP001666
Ruminococcaceae bacterium CPB6	KM454167.2
Clostridium leptum strain DSM 753*	NR_114789.1
Caproiciproducens galactitolivorans strain BS-1*	FJ805840.2
Acetanaerobacterium elongatum strain Z7	AY487928.1
Bacterium NLAEzlC146*	JQ607884.1
Clostridium sp. strain Z6	AY949859.1
*Olsenella profusa**	LC258149.1
*Olsenella umbonata**	FN178462.2
Candidatus *Brocadia anammoxidans*	AF375994.1

*Partial sequence

The role of Ethanol and Lactic acid as electron donors for production of caproic acid

In order to demonstrate the reproducibility of the results depicted in the figure 3, a separate reactor was started-up, inoculated with granular biomass from the fermenter and fed with the same feed. The new fermenter had a total volume of 2.4L, and was operated at 34C, with pH controlled at 5.5, as previously described. The reactor was operated at a HRT of 1 d. The reactor produced caproic acid at a concentration of 4.3±0.6 g L^{-1}. Separate spikes of lactic acid and ethanol (15 g L^{-1}) were applied after a period of starvation aimed at allowing the depletion of the substrates in the feed. After separate spikes with lactic acid (Fig S11, A&B) the concentration of caproic increased, mirroring the consumption of lactic acid.

The volumetric caproic acid production rate in each experiment were 0.48 and 0.40 gC6 L^{-1} h^{-1}, respectively. These are lower than those measured in the previous spike (figure 3) likely due to a lower biomass concentration inside the fermenter. The caproic:lactic acid yields were 0.29 and 0.25 g C6/gLactic acid, respectively. When ethanol was spiked the concentration of all the carboxylic acids remained constant in both replicates (Fig S11, C&D). These results confirm that lactic acid was the preferred electron donor for chain elongation and are in agreement with the results shown in figure 3.

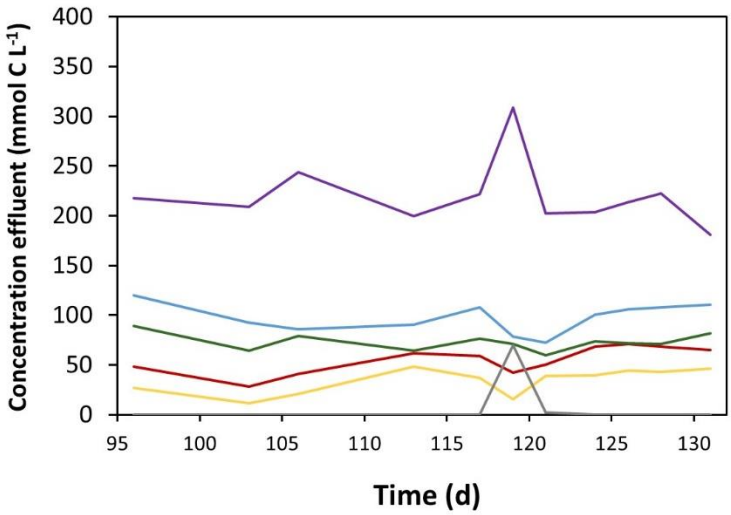

Figure S11. Time course of the evolution of concentration of lactic acid (grey) acetic acid (blue), propionic acid (yellow), n-butyric acid (green), n-valeric acid (red), n-caproic acid (purple), n-heptanoic acid (orange) and n-caprylic acid (black) in the effluent of a second fermenter where the replicates of the ethanol and lactate spikes were carried out.

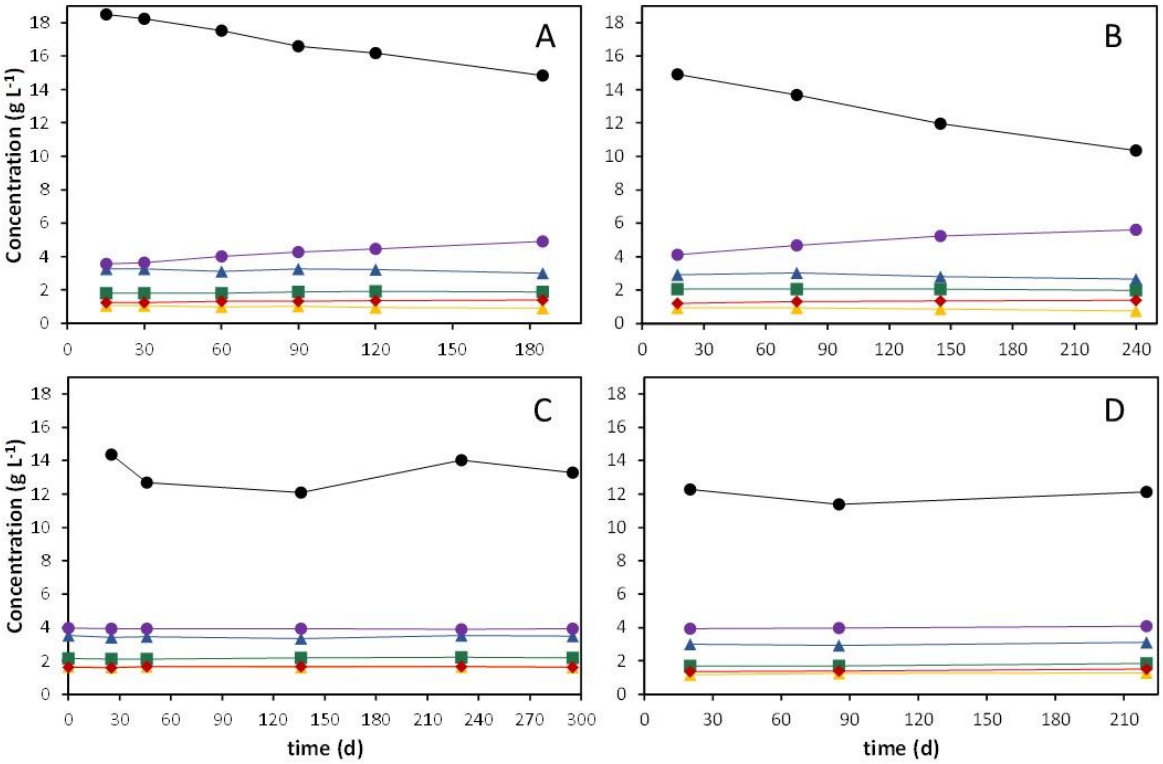

Figure S12. Time course of the evolution of concentration of ethanol and lactic acid (black circles), acetic acid (blue triangles), propionic acid (yellow triangles), n-butyric acid (green squares), n-valeric acid (red diamonds), n-caproic acid (purple circles), n-heptanoic acid (orange circles) and n-caprylic acid (grey circles), after a spike with 15 g lactic acid L^{-1} , added as sodium lactate (Panel A and B) or a spike with 15 g ethanol L^{-1} (Panel C and D).

Environmental sustainability of the process

In order the assess the environmental sustainability of the process, we estimated the waste production and emissions of the overall suggested process.

The thin stillage is a sidestream of the production of bioethanol. After distillation of the ethanol, the bottoms are composed by a water slurry containing the unconverted solids of the fermentation, both suspended and dissolved. The thick solid fraction is separated and used as feed complement due to its high protein and carbohydrate content. The thin fraction (thin stillage) still contains suspended solids (20-40 gTSS L^{-1}) and dissolved solids (ca. 50 g sCOD L^{-1}). This thin stillage is concentrated by evaporating the water. The condensate is reused internally and the solid fraction of the thickened stillage is combined with the previous solid stream and used as feed. In this work with pre-separate the suspended solids of the thin stillage, which contains the largest fraction of the proteins, and use the solid-free thin stillage as feedstock for the fermentation. We leave the solid fraction untouched, which then can still be used as feed complement.

The effluent of the fermentation after extraction of the caproic acid (not applied in our experiment), leaves an aqueous stream that contains most of the carbon in volatile fatty acids, unconverted sugars alcohols and proteins (only about 25% of the carbon is harvested as caproic acid), and organic nitrogen (proteins). In an integrated biorefinery this stream can be used for the production of biogas. In order to evaluate the potential emissions directly derived from the bioconversions of the pipeline, we assumed that the effluent of the fermenter is anaerobically digested generating methane, carbon dioxide and solids. The hydrogen generated as a byproduct of the fermentation can be used as supplementary electron donor for methanogenesis and therefore we assume that all the hydrogen can be converted to methane. The anaerobic effluent can be aerobically treated as an additional polishing step, yielding a treated water stream that can be reused internally, carbon dioxide and a small fraction of aerobic solids. The overall assumed pipeline is depicted in figure S13.

In order to calculate the overall methane, carbon dioxide and sludge yields we assumed:

- The uncharacterized fraction of the COD in the thin stillage is composed by proteins (TKN = 1.38g L^{-1}).

- The dissolved proteins in the stillage have a composition similar to the model protein in bovine serum albumin (BSA). The overall composition of the BSA responds to the formula $C_{2932}H_{4614}N_{780}O_{898}S_{39}$.
- Using BSA as protein model, the recalculated total COD of the thin stillage is 52 g COD L^{-1}, which is similar to the value obtained experimentally (49.9 g COD L^{-1}).
- The recalcitrant fraction of the COD in the thin stillage remains recalcitrant to anaerobic treatment.
- The composition of the biogas in the anaerobic digester is calculated using the Buswell equation.
- 100% of the non-recalcitrant COD is converted to methane.
- 100% of the hydrogen generated during the fermentation is used for production of methane.
- The cell yield in the anaerobic treatment is 0.1 gVSS $gCOD^{-1}$.
- 100% of the COD in the anaerobic effluent is aerobically biodegradable.
- The sludge yield of the aerobic treatment is 0.35gVSS $gCOD^{-1}$.
- The biosolids generated in the aerobic and anaerobic treatment are described by the formula $C_5H_7NO_2$.
- 100% of the produced caproic acid is recovered from the fermentation broth.
- Emissions derived from the operation cannot be derived from the current experiment and are ignored in this calculation.

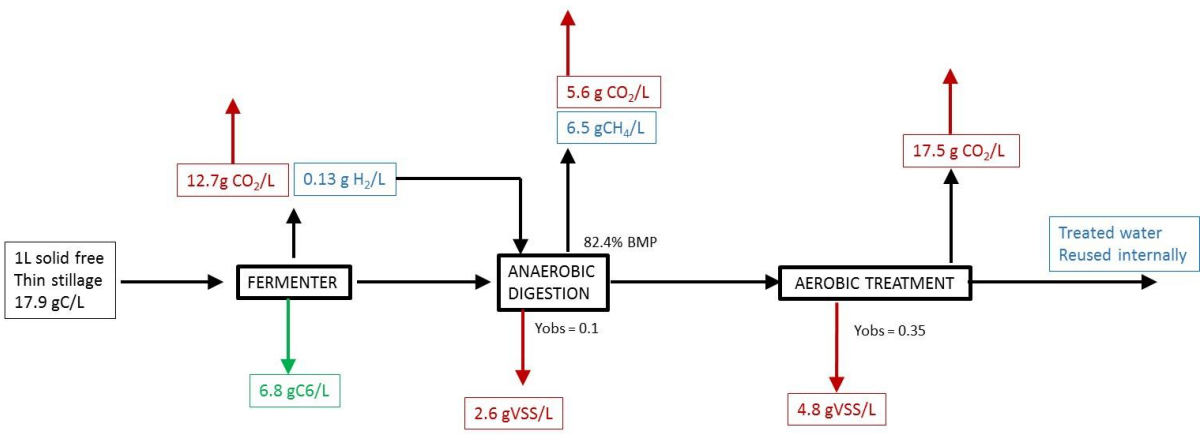

Figure S13. Flow diagram of a process including fermentation of thin-stillage towards caproic acid, and post treatment with anaerobic digestion and aerobic polishing. The main intended product is

caproic acid (green), the blue boxes show valuable products to be used internally (H_2, CH_4 and water). The waste streams are indicated in red boxes (CO_2 and sludge).

In the proposed pipeline, 6.8 g of caproic acid are generated per liter of solid-free thin stillage. Methane (6.5 g CH_4/Lstillage), is generated during anaerobic digestion. Methane has a lower heating value of 50J/g. Sludge (7.44 gVSS/gC6) and carbon dioxide (5.26 g CO_2/gC6) are generated during the fermentation and treatment of the fermentation effluent.

NMR spectra of caproic and caprylic acids

The H1 and 13C shifts for caproic and caprylic acids can be found in the websites below. These don't interfere with the anomeric or bulk polysaccharide regions that we based our assessment on.

http://www.bmrb.wisc.edu/metabolomics/mol_summary/show_data.php?id=bmse000351&whichTab=1

http://www.bmrb.wisc.edu/metabolomics/mol_summary/show_data.php?id=bmse000502

References

1. Nielsen, S. S. (2010). Phenol-Sulfuric Acid Method for Total Carbohydrates. Food Analysis Laboratory Manual. S. S. Nielsen. Boston, MA, Springer US: 47-53.
2. R. Vilchez-Vargas, R. Geffers, M. Suárez-Diez, I. Conte, A. Waliczek, V. S. Kaser, M. Kralova, H. Junca and D. H. Pieper, *Environmental Microbiology*, 2013, **15**, 1016-1039.
3. A. Klindworth, E. Pruesse, T. Schweer, J. Peplies, C. Quast, M. Horn and F. O. Glöckner, *Nucleic Acids Research*, 2013, **41**, e1-e1.
4. P. D. Schloss, S. L. Westcott, T. Ryabin, J. R. Hall, M. Hartmann, E. B. Hollister, R. A. Lesniewski, B. B. Oakley, D. H. Parks, C. J. Robinson, J. W. Sahl, B. Stres, G. G. Thallinger, D. J. Van Horn and C. F. Weber, *Applied and Environmental Microbiology*, 2009, **75**, 7537-7541.
5. J. J. Kozich, S. L. Westcott, N. T. Baxter, S. K. Highlander and P. D. Schloss, *Applied and Environmental Microbiology*, 2013, **79**, 5112-5120.
6. Q. Wang, G. M. Garrity, J. M. Tiedje and J. R. Cole, *Applied and Environmental Microbiology*, 2007, **73**, 5261-5267.